PRACTICAL ASPECTS OF FATIGUE ANALYSIS OF A WELDMENT

K. Yamada* and P. Albrecht**

INTRODUCTION

Calculations of fatigue crack propagation based on the fracture mechanics approach have been shown to yield good correlation between observed and predicted number of cycles required to extend a fatigue crack from an initial size to a final size. The results are particularly encouraging when the experiment is done with standardized specimens, such as the compact tension specimen, for which an accurate expression for the stress intensity factor is available and the crack growth rates can be measured.

Many uncertainties are introduced when the approach is applied to fatigue life prediction of structural components subjected to a service stress history. Among the factors which need special consideration are initiation life, load interaction, crack shape, weldment and geometry irregularities, growth rates and crack closure effects. The objective of this paper is to discuss some of these aspects in relation to fatigue test data for a non-load carrying fillet weld.

EXPERIMENTAL WORK

The 27 tensile specimens tested in this study were saw-cut from a larger plate which had transverse stiffeners continuously welded by the automatic submerged arc process. The cross-section of the main plate was 10 mm by 26 mm and the leg size of the welds were 7 mm, as illustrated in the insert to Figure 1. The detail simulates the stress condition at transverse stiffeners welded to the web and the flange, as well as diaphragm gussets attached to bridge girder webs. All steel was ASTM A588 with 420 MPa yield strength and 566 MPa tensile strength.

The non-dimensionalized stress histogram employed in the variable amplitude fatigue tests of all specimens is shown schematically in the insert to Figure 3. It is broken down into 10 constant amplitude stress range bars with a frequency distribution corresponding to the upper half of the average of 106 strain histories recorded by many investigators on highway bridges throughout the United States [1]. The stress range bars were arranged in one random order and then factored to yield the three levels of variable amplitude stress range: (a) 103 to 307 MPa, (b) 152 to 304 MPa, and (c) 193 to 386 MPa. The stress history was applied repeatedly in blocks of 10,000 cycles or less.

At a preselected number of cycles, the weld toes of all specimens were brushed with Dykem Steel Blue dye in order to mark the extent of fatigue cracking at that time. The dye-marked crack length, a, are plotted in Figure 1 against the number of cycles non-dimensionalized by the fatigue

*Nagoya University, Nagoya, Japan.
**University of Maryland, College Park, Maryland, U.S.A.

life of the specimen. When the dye was applied before some 40 percent of the fatigue life had ellapsed, markings were usually not visible, as indicated in Figure 1 by the open circles with arrows.

ANALYSIS

In this study, analysis of crack propagation was confined to the number of cycles required to grow the crack from that size at which the weld toes were dyed to failure. For the smallest combination of marked crack length and stress range the computed value of the stress-intensity factor range was $\Delta K = 6.1$ MPa$\cdot$m$^{1/2}$, that is more than the threshold value $\Delta K \simeq 5$ MPa$\cdot$m$^{1/2}$ for structural steels. Consequently, a log-log linear crack growth equation of the form

$$\frac{da}{dN} = 48 \times 10^{-10} \Delta K^3 \qquad (1)$$

was assumed. Deviations from this straight line, as the K value at the peak of the stress cycle approaches the fracture toughness of the material, need not be considered because at that time less than one percent of the fatigue life remain. Any errors on such a small quantity would be insignificant.

The range of the stress-intensity factor for the deepest point of the semi-elliptical crack front was computed from:

$$\Delta K = \frac{1.12}{E_k} F_G \sigma_r \sqrt{\pi a} \sqrt{\frac{W}{\pi a} \tan \frac{\pi a}{W}} \qquad (2)$$

Equation (2) is based on the widely used ΔK estimate for a semi-elliptical surface crack in a flat plate. It was modified by a geometry correction factor, F_G, which accounts for the stress concentration effect of the weld geometry [2]. Equation (1) was integrated numerically by the Runge Kutta method for the crack extension on a cycle by cycle basis. The results of the analysis for all three variable amplitude stress range levels are plotted in Figure 3 as bands bounded on the left and right by assumed constant semi-axis ratios of a/b = 0 (half-tunnel crack) and a/b = 1/3, respectively. Any point on the curves gives the computed number of cycles of crack propagation from that crack length to failure and the data points correspond to the observed number of cycles from the dye-marked length to failure.

Figure 4 compares the computed and observed number of cycles. Both figures indicate good correlation for all three stress range levels when the number of cycles were small in proportion to the total fatigue life. The shorter the crack length, the more the model underestimated the observed number of cycles. The errors were in general on the safe side.

DISCUSSION

Crack Initiation and Propagation

The total fatigue life equals the sum of the number of cycles required to initiate a crack and the cycles needed to propagate it to failure. Crack propagation models can, obviously, only predict the latter stage and may be applied to the computation of crack extension for those cycles of the variable amplitude history for which the combination of stress range and

crack size gives values of ΔK larger than ΔK_{th}. This was the case for all data points plotted in Figure 1. The trend of the data shows that the propagation life for this specimen amounted to some 60 percent, at least, of the total number of cycles to failure. Hence, the major portion is tractable by analysis.

Some attempts of predicting the crack initiation life at notches, as a function of stress range and stress concentration factor or notch radius, were reported in the literature [3]. But, extension of this approach to typical structural details with sudden transitions in geometry and theoretically infinite stress concentrations needs to be demonstrated.

Crack Shape

The depth, a, and the half-width, b, of the part-through cracks at the weld borders are plotted in Figure 2. The solid circles indicate the dye-marked cracks and the open circles represent those found in the weld toe plane at the opposite side of the main fracture, exposed after the test, and also from a previous study [4].

The data reflects a wide range of aspect ratios extending from a/b = 1/2 to cracks of nearly half-tunnel shape for which the crack width b equals the 26 mm specimen width. This variation was found at all observed crack lengths.

Also plotted with X symbols are aspect ratios for part-through cracks at toes of manually welded transverse stiffeners [5]. The manual welds are more prone to defects and weld bead irregularities which act as starting points for single run-away cracks of higher aspect ratio. Automatic welding, on the other hand, produces more regular welds with smoother borders. This tends to prolong the initiation life, enhances multiple crack initiation, and results in lower aspect ratios. For analysis purposes in this study, ratios of a/b = 1/3 and a/b = 0 were chosen. Consequently, values for the complete elliptical integral in equation (2) of $E_k = 1.11$ and $E_k = 1.0$, respectively were obtained and the results of the analysis were affected as shown by the bands in Figure 3.

K-computation

The expression for the stress intensity factor given by equation (2) is approximate in that it neglects, for example, interaction effects between the free surface, finite width and geometry correction factors. But it provides a simple, rapid and adequately accurate solution for K values at structural details. Actual weld shapes differ from the idealized 45 degree shape by the concavity/convexity of the bead, variations in leg size, undercut, ripples, and irregularities at stop-start positions. Such differences occur from one weld to another and greatly influence the weld border stress field over a depth of about one tenth of the plate thickness where a major part of the fatigue life is typically spent.

Although advanced three-dimensional finite element algorithms for K-computation are available, the need to repeat the calculations for many fatigue crack sizes does not justify this approach from an economy viewpoint. Further, any potential gain in accuracy would have to be weighed against the effect of geometrical weld bead variations, and may well be illusory.

Load Interaction

Load interaction occurs in high-low stress range sequences while the crack front driven by the low stress range cycles, penetrates the larger plastic zone formed under the prior high load excursion. The clamping effect of the surrounding elastic stress field on the enlarged crack tip plastic zone increases the residual compression stresses and slows down the crack growth rate at the lower stress range. Appreciable enhancement of growth is not known to occur in low-high load sequences.

Fatigue life extension is enhanced, the deeper the crack grows into the plastic zone of the prior high load excursion. A measure of the length of interaction is given by the ratio of undelayed crack growth Δa, computed directly from equation (1) for small ΔN values, and the overload plastic zone diameter

$$2r_y = \frac{1}{\pi}\left(\frac{K}{\sigma_y}\right)^2 \qquad (3)$$

It can be shown that the ratio of $\Delta a/2r_y$ is proportional to ΔN and ΔK at the low stress range cycling. Except for one specimen, this ratio did not exceed 6 percent whereas several investigators have shown that the crack must penetrate a single overload plastic zone by some 10-15% before the delay mechanism becomes fully effective. Furthermore, in variable amplitude block loading the peak stresses are sufficiently close to create a rather uniform envelope of all plastic zones, in contrast to constant amplitude tests with widely spaced overloads. This reduces variations in clamping effects and decreases delay effects. In this study, variations in block size from 100 to 10,000 cycles were found to have a statistically insignificant effect on total fatigue life.

Crack Growth Rates

The crack propagates in a plane through the weld toe, about normal to the applied loads, and is therefore embedded in the heat affected zone. Except for a few exploratory studies, measurements of crack growth rates in heat affected zones along weld borders are not available. One must therefore use data for plain material. Equation (1) gives average growth rates in the range 15 MPa$\cdot$m$^{1/2}$ < ΔK < 60 MPa$\cdot$m$^{1/2}$ for four ferritic steels [6] and correlates well with the very slow growth rates in the range 5 MPa$\cdot$m$^{1/2}$ < ΔK < 10 MPa$\cdot$m$^{1/2}$ reported by Paris [7] for 9310 steel. Inspite of the careful experimental techniques, the data for the four ferritic steels were bound by two lines located at a factor of 1.5 above and below the mean line. The effect of this variation on fatigue life estimates is not insignificant.

Crack Closure

The crack closure effect that is the impingement of crack surfaces occurs when residual deformations in the wake of the advancing crack front cause the surfaces to contact and prevent complete relaxation of crack tip stresses at zero load. Experimental evidence shows that a portion of the stress cycle is needed to open the crack. Just how important the crack closure phenomenon is, becomes apparent from Elber's data for 2024-T3 aluminum alloy [8]. For a minimum to maximum stress ratio of R = 0, he found that the effective range of the stress intensity factor was one half of the nominal value in equation (1). Since crack growth rates of structural steels are related to the third power of ΔK, any crack closure effect on

the numerical value of ΔK is greatly magnified when it comes to fatigue life computation. Unfortunately, quantitative studies of crack closure have not yet been done for structural steels and their results cannot be implemented.

In welded structures, the problem is further complicated by the stress concentration and the residual tensile welding stresses at the weld toe. For the specimens and loads in this study, simple computations suggested that the combined effect of stress concentration ($K_t \approx 2.5$) and residual welding stresses caused the material at the weld toe to yield to a depth of 0.3 to 1 mm. Note that 2/3 of all marked cracks had a depth of less than 1 mm. Also, Figure 4 shows that for each stress range level the smaller the dye-marked crack length, and hence the longer the life, the more the observed number of cycles exceeds the computed value. This trend is attributed to the length of time a crack is growing through regions of residual deformations and subjected to closure effects. At present, there is no way of accounting for these effects at the application level.

REFERENCES

1. YAMADA, K. and ALBRECHT, P., 55th Annual TRB Meeting, Washington, D.C., 1976.
2. ALBRECHT, P. and YAMADA, K., Journal of the Structural Division, ASCE, 1976.
3. BARSOM, J. M. and McNICOL, R. C., 7th National Symposium on Fracture Mechanics, University of Maryland, MD., 1973.
4. ALBRECHT, P., ABTAHI, A. and IRWIN, G. R., Civil Engineering Report, University of Maryland, MD., 1976.
5. ALBRECHT, P., Ph.D. dissertation, Lehigh University, Pa., 1972.
6. BARSOM, J. M., First National Conference on Pressure Vessels and Piping, San Francisco, California, May, 1971.
7. PARIS, P. C., Closed Loop, MTS System Co., 2, 1970.
8. ELBER, W., ASTM STP 486, ASTM, 1971.

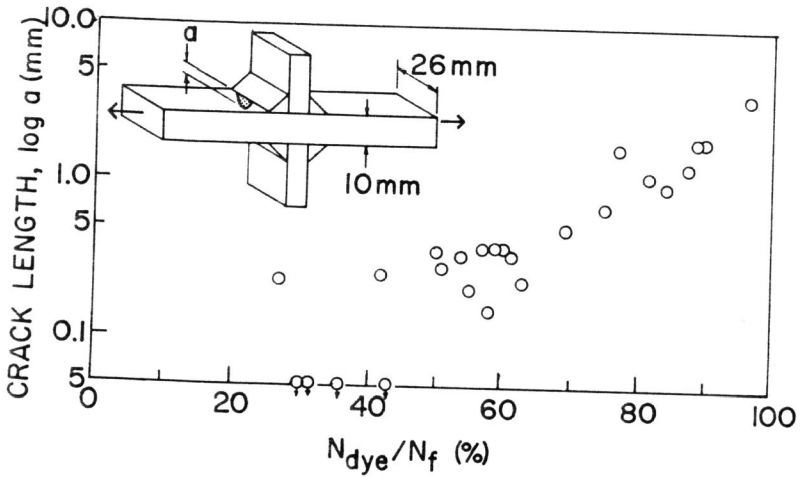

Figure 1 Relation between dye-marked crack length and number of cycles.

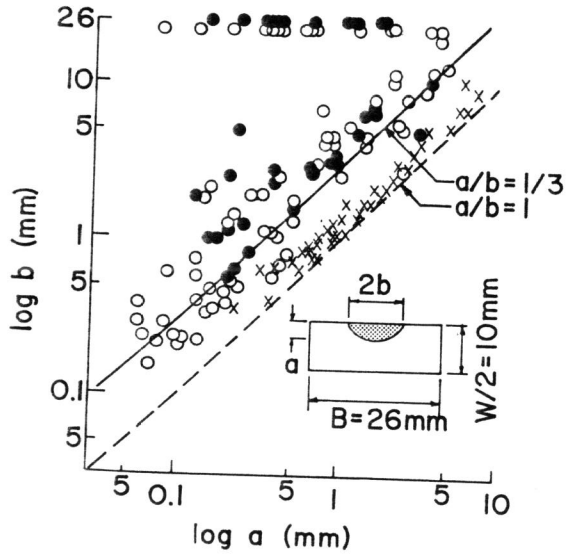

Figure 2 Aspect ratio of surface cracks at weld toe.

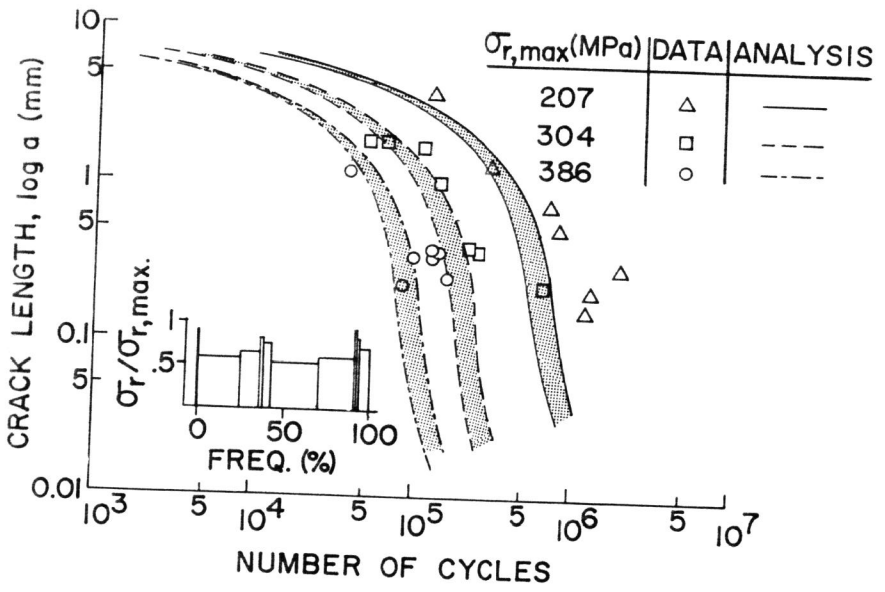

Figure 3 Results of crack propagation analysis.

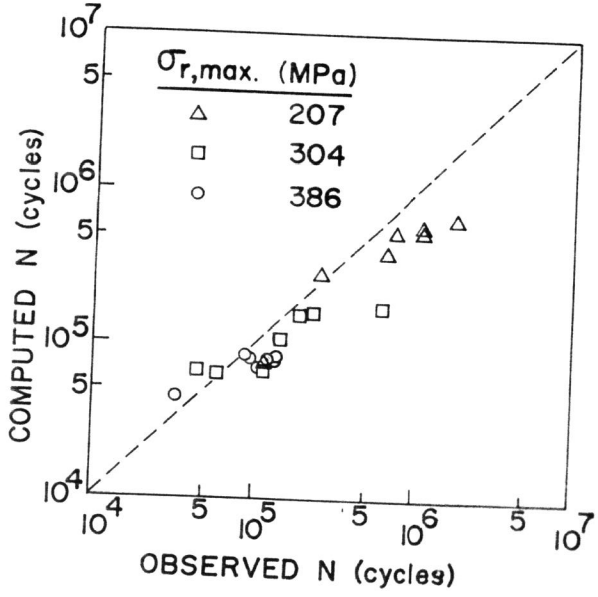

Figure 4 Comparison between observed and computed number of cycles from dye-marked crack length to failure.